SAND2020-1764PE

Molecular dynamics study of shock compression in porous silica glass

Keith Jones, J. Matthew D. Lane, Tracy Vogler

Sandia National Laboratories. Albuquerque, NM and Livermore, CA.

Sandia National Laboratories is a multimission laboratory managed and operated by National Technology & Engineering Solutions of Sandia, LLC, a wholly owned subsidiary of Honeywell International Inc., for the U.S. Department of Energy's National Nuclear Security Administration under contract DE-NA0003525.

Motivation for studying porous silica

Low density silica aerogels with a range of initial densities are commonly used in extreme conditions:

- Space missions
- High P research

Gaining a more detailed understanding of the processes occurring under these conditions is important.

Validate model by comparison with experiment.

Experimental data

M. Burchell et al., *Annu. Rev. Earth Planet. Sci.* **34**, 385 (2006).
D. Brownlee et al., *Science* **314**, 1711 (2006).
M. D. Knudson, J. R. Asay, and C. Deeney, *J. Appl. Phys.* **97**, 073514 (2005).
N. Holmes, High-Pressure Science and Technology—1993 (AIP, New York, 1994), p. 153.
M. D. Knudson and R. W. Lemke, *J. Appl. Phys.* **114**, 053510 (2013).

Motivation for studying porous silica

A density inversion in the Hugoniot is observed experimentally at high shock pressures for highly porous silica. This is due to shock energy being converted into kinetic energy as particles are vaporized into the void space. Thermal expansion occurs with respect to the same system shocked to a lower pressure. Local heating during void collapse has been studied with molecular dynamics (MD).

Can we model this density inversion with molecular dynamics?

Can we model this density inversion without using the expensive, propagating, non-equilibrium molecular dynamics (NEMD) model for dynamical shock simulation?

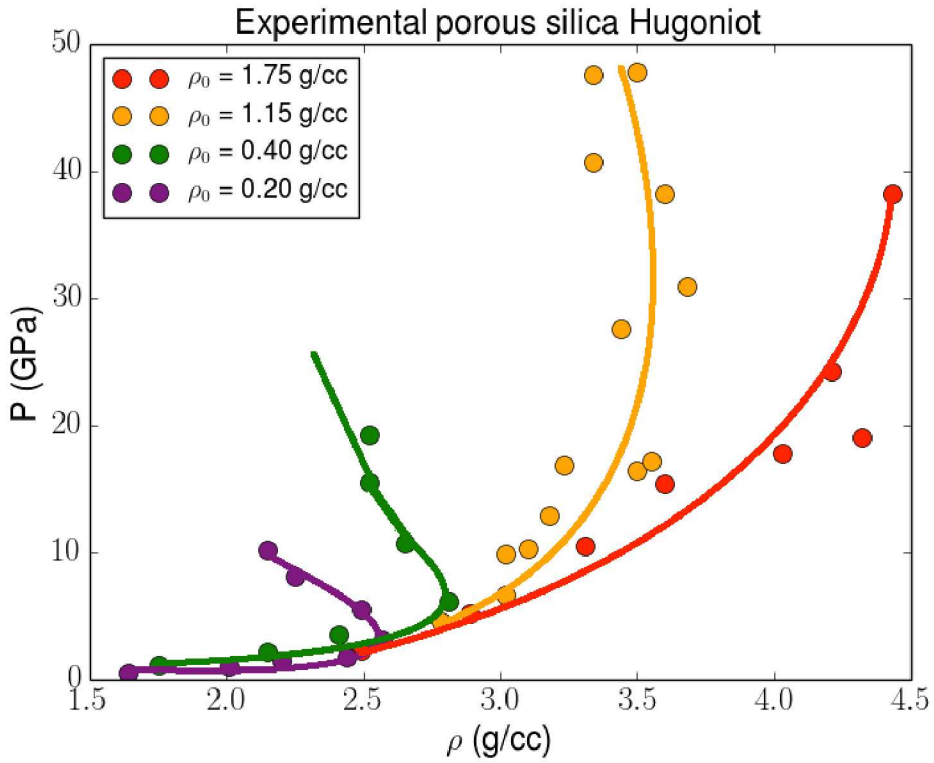

Density inversion in highly porous silica Hugoniot is not well studied with MD.

R. F. Trunin, *Experimental data on shock compression and adiabatic expansion of condensed matter* (2001).

J. Matthew D. Lane et al., *Comp. Mat. Sci.* ***79****, 873-876 (2013).*

Methodology - General

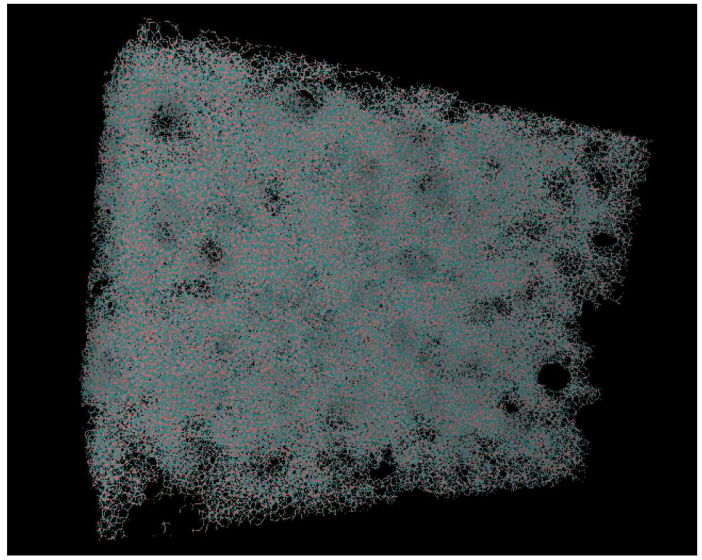

Initial density	Porosity
2.212 g/cc	0 %
2.09 g/cc	~5 %
1.08 g/cc	~50 %
0.56 g/cc	~75 %
0.23 g/cc	~90 %
0.14 g/cc	~95 %

A range of silica systems with various porosities (initial densities) have been created in LAMMPS, molecular dynamics package.

Molecular dynamics at the fully atomistic level is employed. Each atom is treated as a partially charged point particle moving under the influence of a user specified potential energy surface:

Short/medium range interactions are calculated using the SiO_2 BKS potential, a simple, tabulated interatomic potential for silica.
Long range interactions are calculated using an Ewald summation.

Each porous silica system is shocked to a range of pressures from the reference state in order to build the Hugoniot.

S. Plimpton, *J. Comp. Phys.* **117**, 1-19 (1995).
B. W. H. van Beest et al., *Phys. Rev. Lett.* **64**(16), 1955 (1990).

Methodology – The Hugoniot in MD

Hugoniot: the locus of points representing a series of final, shock states originating from a single reference state.

$$(E_1 - E_0) = \frac{1}{2}(P_1 + P_0)(V_0 - V_1)$$

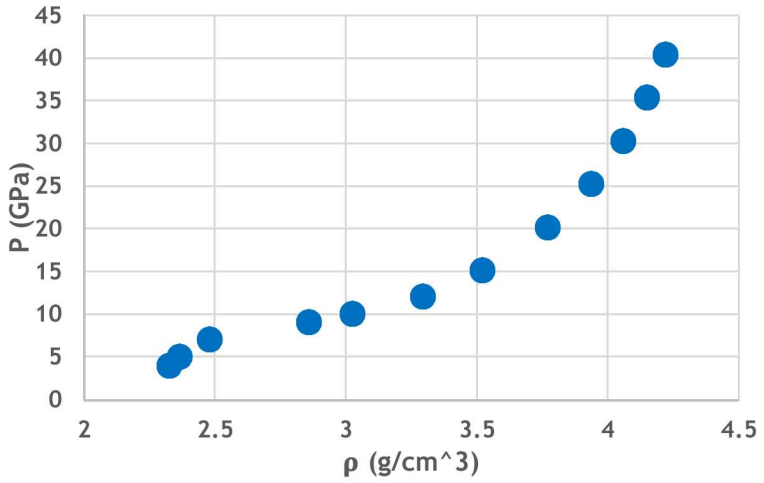

Reproducing the final state in MD

1. Non-equilibrium molecular dynamics. Propagate a shock through the material via a momentum mirror, calculate state variables to verify jump conditions.
   - Expensive and requires large system sizes.
   - Effectively reproduces experimental Hugoniot data for porous systems.

2. Non-propagating, constant stress Hugoniostat method. Uniaxially compress system until the final pressure is reached and jump conditions are met.
   - Less expensive.
   - Well tested in traditional Hugoniot space.
   - Not guaranteed to evolve along Rayleigh line or any other path through ρ, P space.
   - Path and efficiency of path depend on damping coefficients.
   - Previously validated on 50% porous silicon.

J. Matthew D. Lane et al., AIP Conf. Proc. **1793**, 120010 (2017).
B. L. Holian and P. S. Lomdahl, *Science* **280**, 2085 (1998).
R. Ravelo et al., *Phys. Rev. B* **70**, 014103 (2004).

Methodology – The Hugoniot in MD

75 % porous (0.56 g/cc) silica.
Final pressure: 30 Gpa.
Time step: 0.2 fs.

System gets very hot (~15000 K) for MD, compared to an analogous final pressure for fully dense silica (~2000 K). Final state is not very sensitive to damping coefficient ratios.

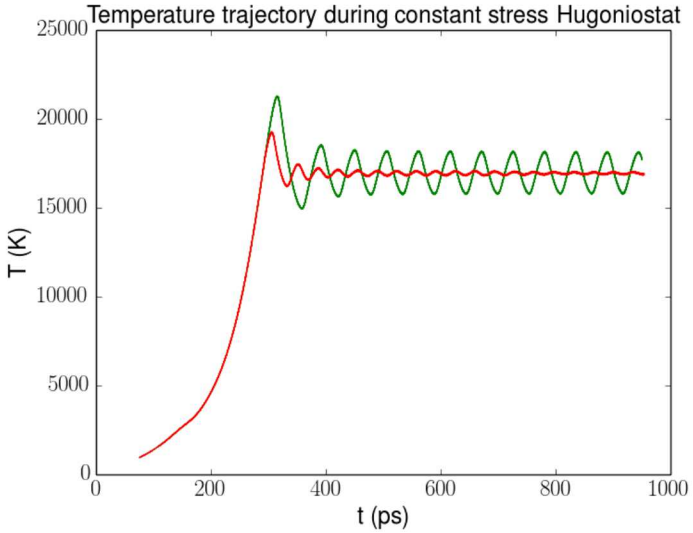

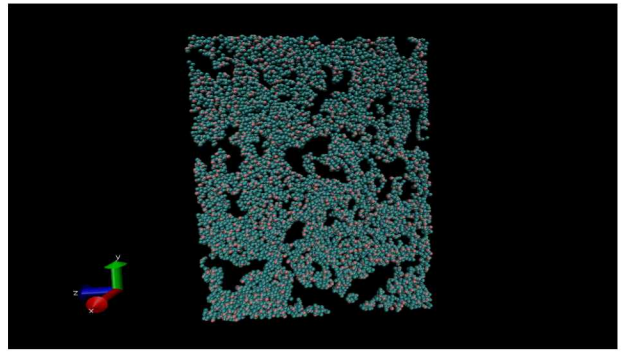

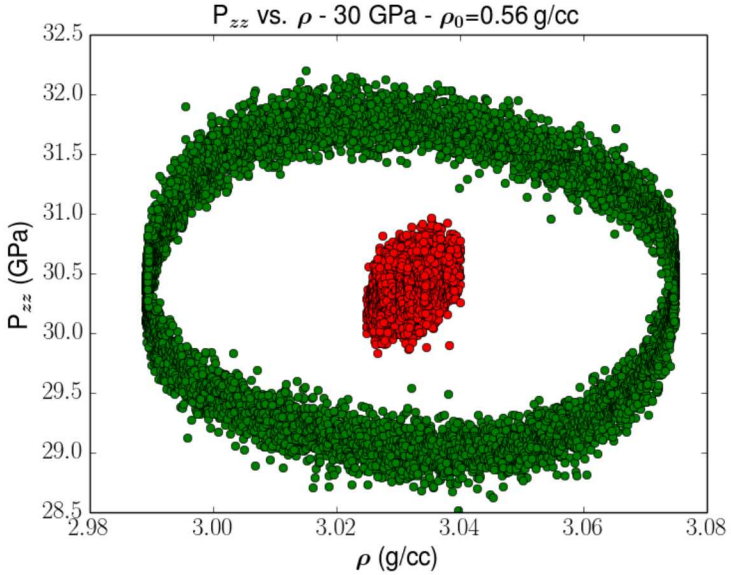

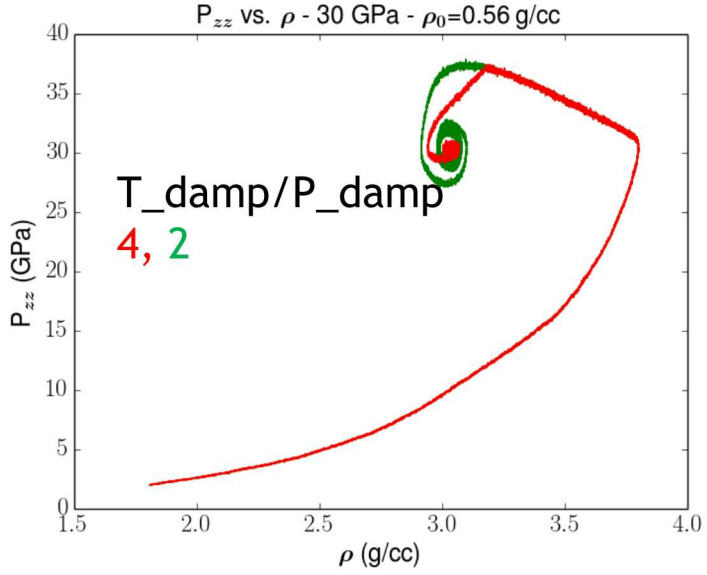

Results – Density inversion

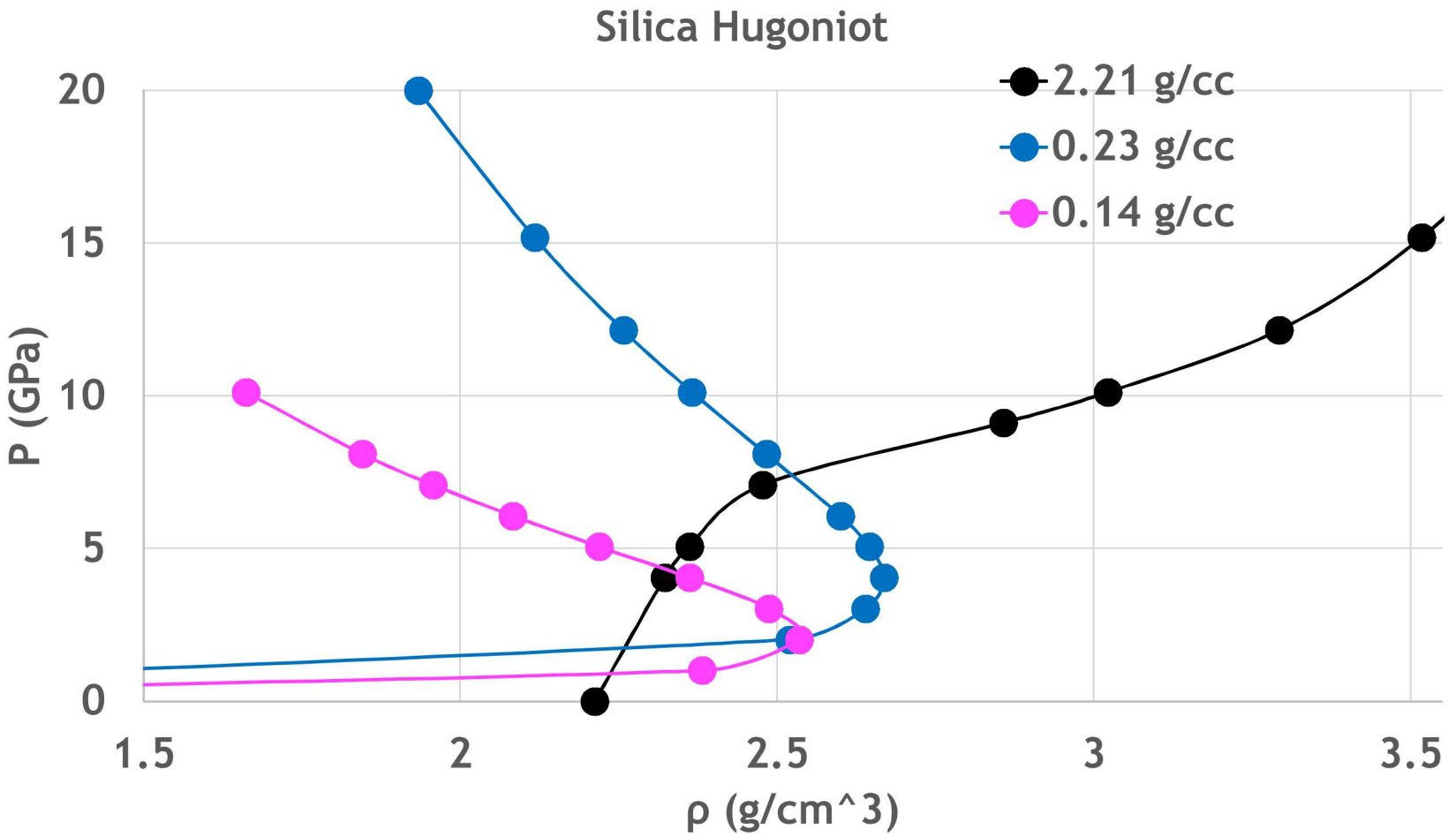

Demonstrated density inversion is in qualitative agreement with experiments

Results – Density inversion

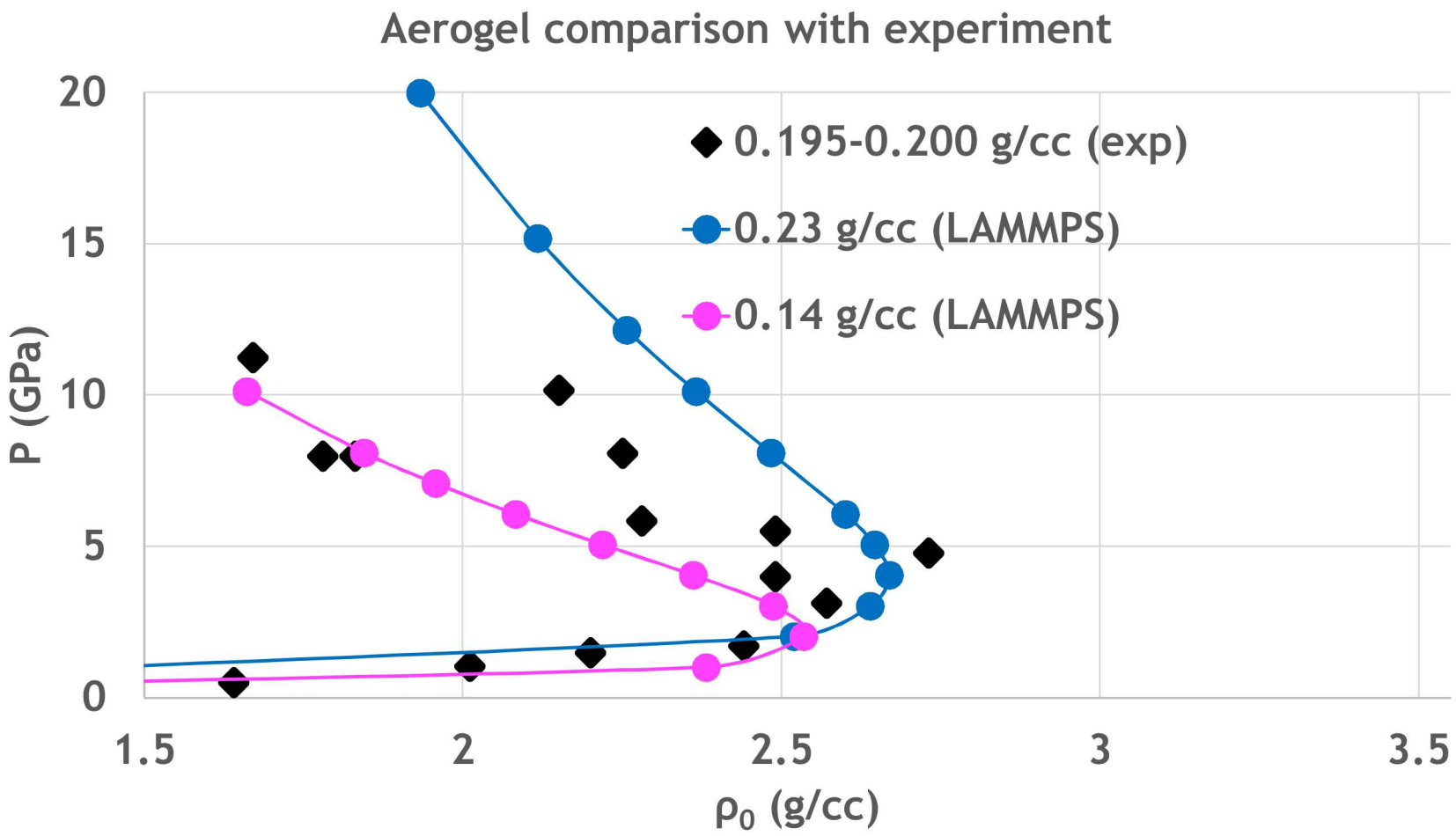

R. F. Trunin, *Experimental data on shock compression and adiabatic expansion of condensed matter* (2001).

Results – Density inversion

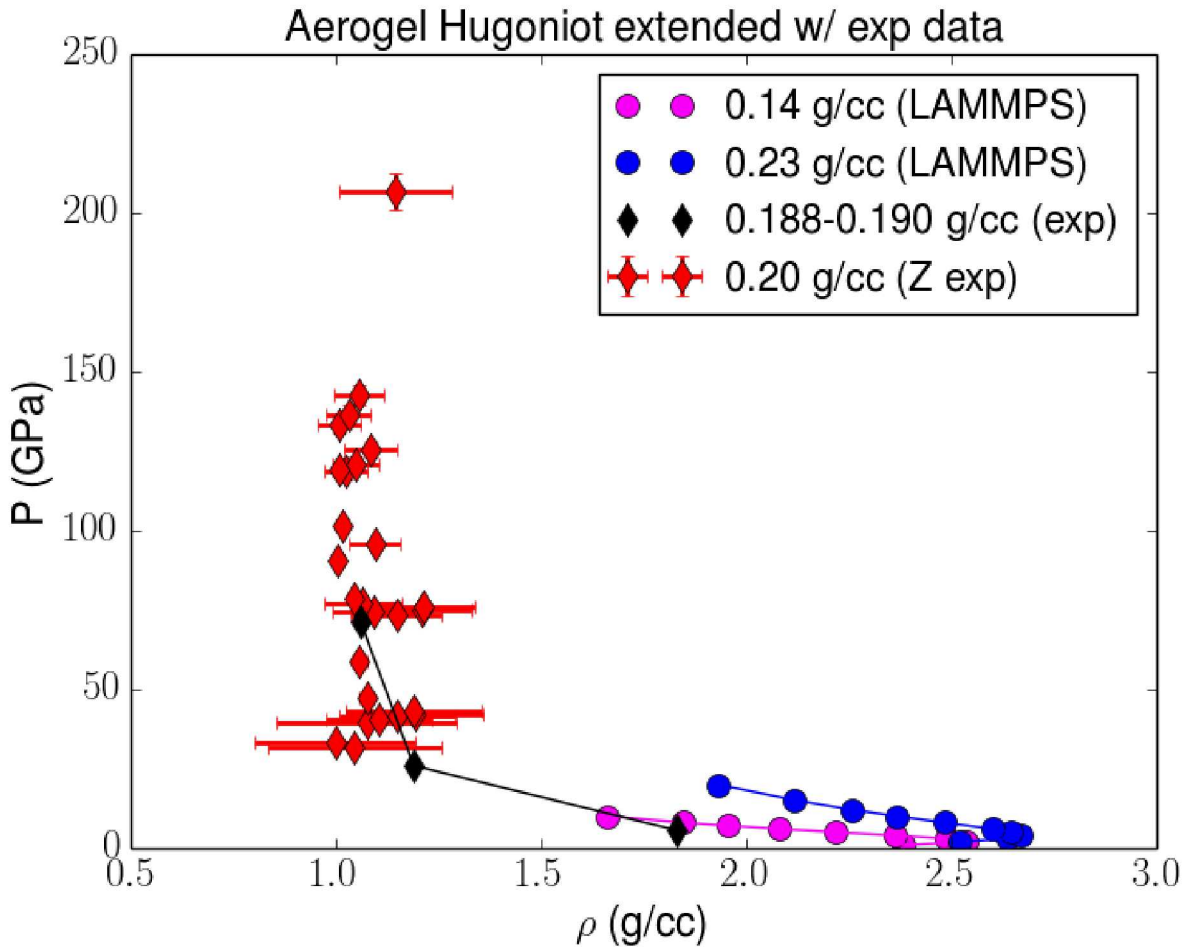

Very high pressure experimental data for highly porous silica, collected using the Z-machine, plotted against LAMMPS and other experimental data shows a cusp in the Hugoniot.

Z machine data is not reproducible with molecular dynamics. Simulation at the level of density functional theory is needed.

M. D. Knudson and R. W. Lemke, *J. Appl. Phys.* **114**, 053510 (2013).
R. F. Trunin, *Experimental data on shock compression and adiabatic expansion of condensed matter* (2001).

Conclusions

BKS, a very simple SiO_2 potential, coupled with the constrant stress Hugoniostat reproduces the Hugoniot for porous SiO_2.

Negative dP/dρ in the Hugoniot for highly porous SiO_2 is qualitatively captured in this very simple model.

Acknowledgements

Sandia National Labs
- High Performance Computers

Kyle Cochrane

Thomas Mattsson

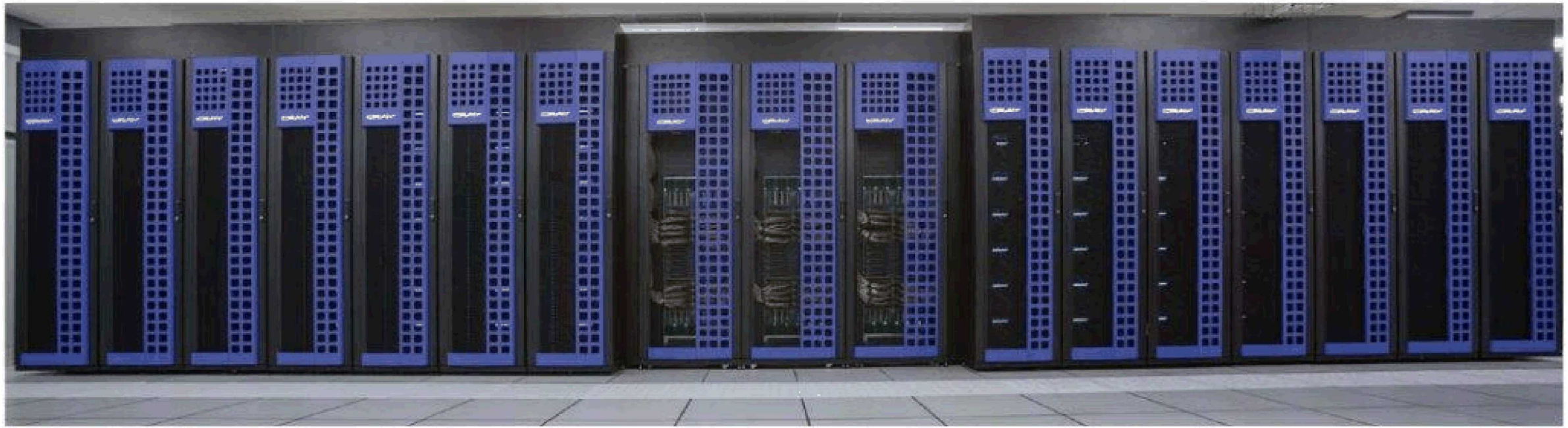

Phenolic polymer pyrolysis via reactive molecular dynamics simulation

PRESENTED BY

Keith A. Jones, J. Matthew D. Lane, Nathan W. Moore

Sandia National Laboratories is a multimission laboratory managed and operated by National Technology & Engineering Solutions of Sandia, LLC, a wholly owned subsidiary of Honeywell International Inc., for the U.S. Department of Energy's National Nuclear Security Administration under contract DE-NA0003525.

Rationale

Phenolic polymer is an ablative material commonly used in thermal protection systems (TPS).

Many TPS models are empirically based, limiting their scope of accuracy.

Chemical degradation of phenolic is a key precursor to TPS ablation.

Atomistic simulations have the potential to improve ablation models.

We seek to develop a thermokinetic model for phenolic pyrolysis informed by molecular dynamics simulations.

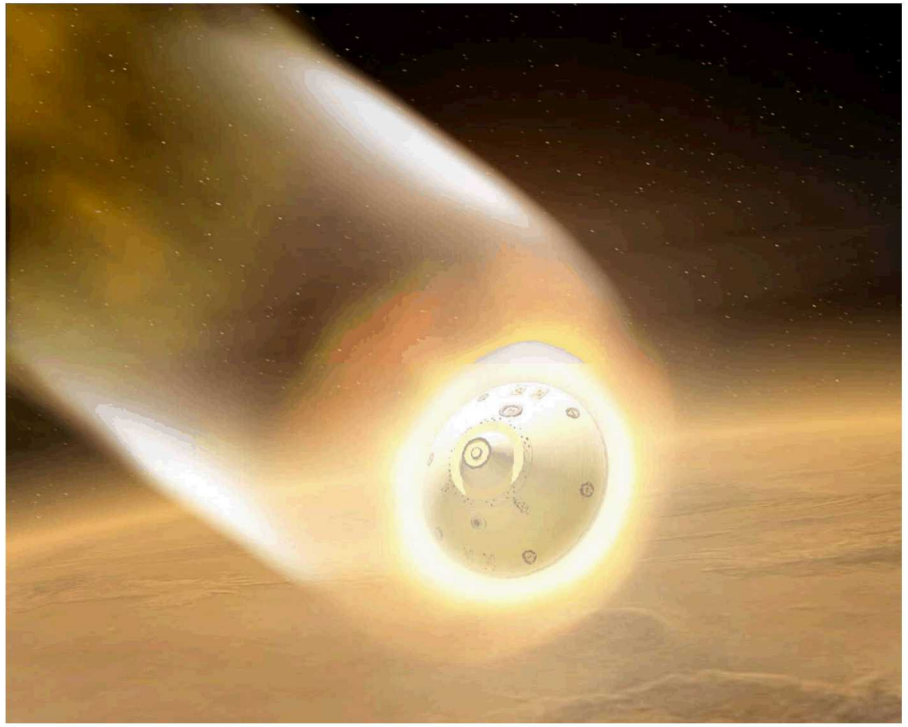

https://mars.nasa.gov/resources/2071/mars-exploration-rovers-entering-the-mars-atmosphere/?site=insight

Introduction

Phenolic polymers

- Key components in carbon composites in heat shields in extreme environments.
- Can vary greatly, depending on curing conditions, in crosslink extent, initial density, stoichiometry, molecular structure.

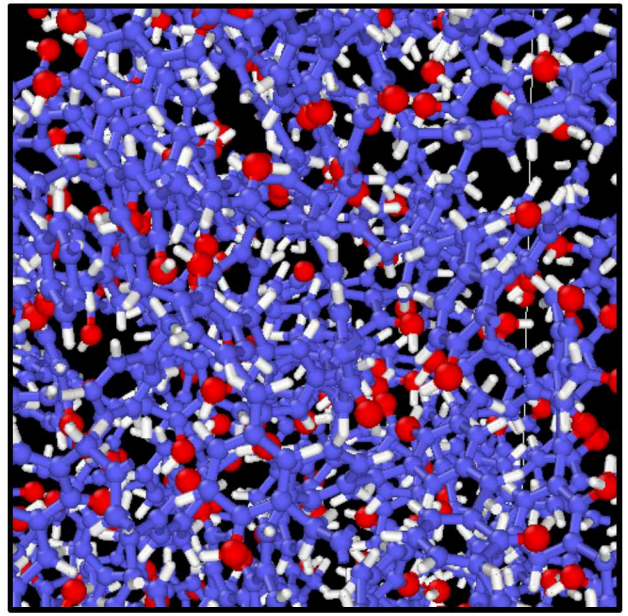

Reactive molecular dynamics (MD) can provide insight into
-Processes that occur during pyrolysis.
-The relationship between molecular structure, density, and pyrolytic breakdown.

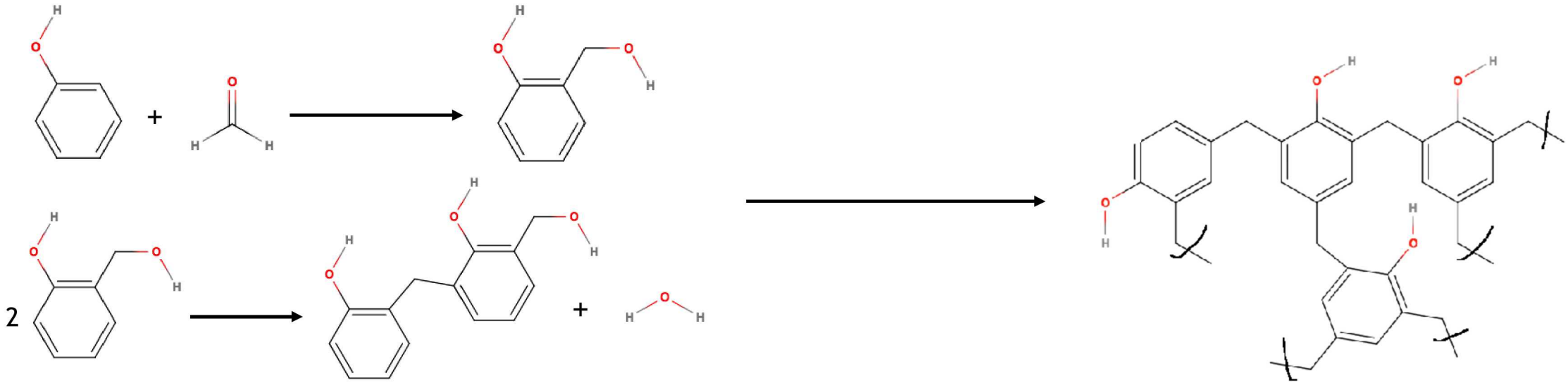

J. B. Scoggins et al. *Aerospace Sci. and Tech.* **66**, 177-192 (2017).

Reax parametrizations

ReaxFF – Bond order MD potential that handles chemistry.
Various parametrizations for different combinations of atoms under different conditions.

We studied phenolic pyrolysis with 3 different ReaxFF parametrizations using the LAMMPS MD package:

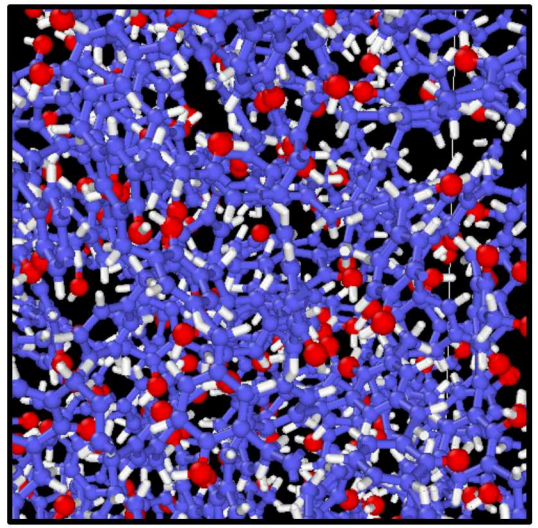

1.) CHO – commonly used for hydrocarbon reactivity.

2.) Mattsson – Past success simulating polymers under chemistry-inducing shock (up to 60 GPa). Well tested for systems containing H and C.

3.) Hybrid parametrization – Mattsson parametrization utilizing the O-H---O hydrogen bonding parameters from CHO introduced to capitalize on the strengths of the other two.

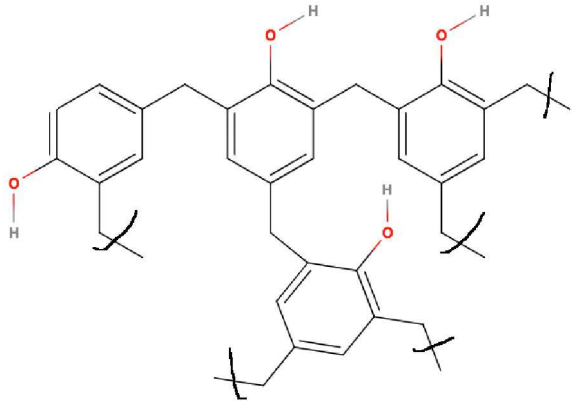

S. Plimpton *J. Comp. Phys.* **117**, 1-19 (1995).
A. C. T. van Duin et al. *J. Phys. Chem.* **105**, 9396-9409 (2001).
K. Chenoweth et al. *J. Phys. Chem. A* **112**, 1040-1053 (2008).
A. Harpale et al. *Carbon* **130**, 315-324 (2018).
T. R. Mattsson et al. *Phys. Rev. B* **81**, 054103 (2010).
J. Matthew D. Lane and N. W. Moore *J. Phys. Chem. A* **122**, 3962-3970 (2018).

Phenol density at various temperatures

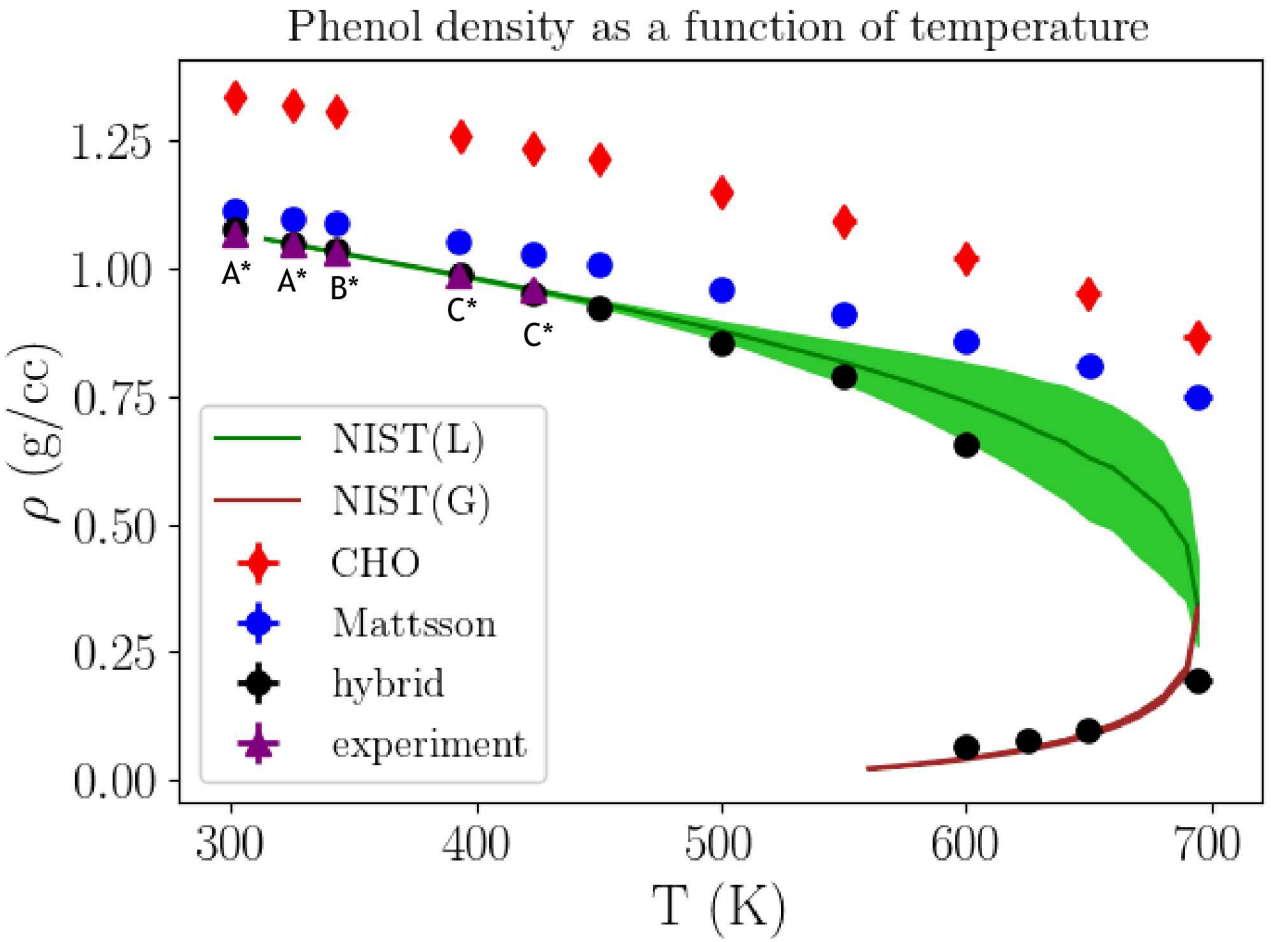

Hybrid agrees with experiment and the NIST model to a greater degree than the parametrizations from which it was derived.

Phenol equilibration - various points in P,T space along L/G coexistence curve.

Phenol data extracted from NIST web thermo data tables – derived from ThermoData Engine.

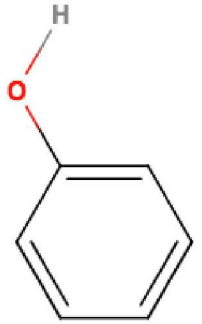

Phenol

A* R. B. Badachhape et al. *J. Chem. And Eng. Data* **10**, 143 (1965).
B* D. L. Cunha et al. *J. Chem. Eng. Data.* **58**, 2925-2931 (2013).
C* C. A. Buehler et al. *J. Am. Chem. Soc.* **54**(6), 2398-2405 (1932).
E.W. Lemmon et al. 2018 https://dx.doi.org/10.18434/T4JS3C
J. Chem. Inf. Model. **45**, 816-838 (2005).
J. Chem. Inf. Model. **47**, 1713-1754 (2007).
J. Chem. Inf. Model. **49**, 503-517 (2009).
J. Chem. Inf. Model. **49**, 2883-2896 (2009).

Phenolic pyrolysis activation energies

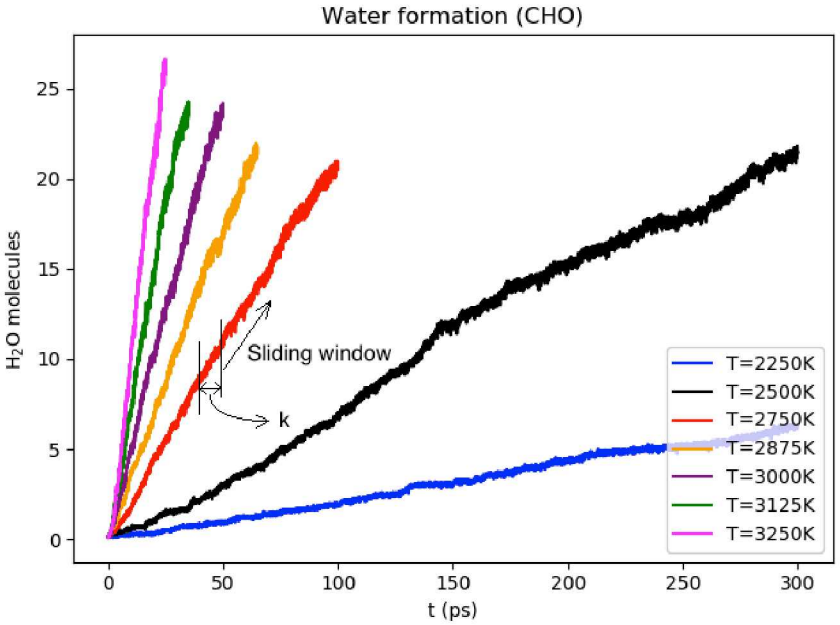

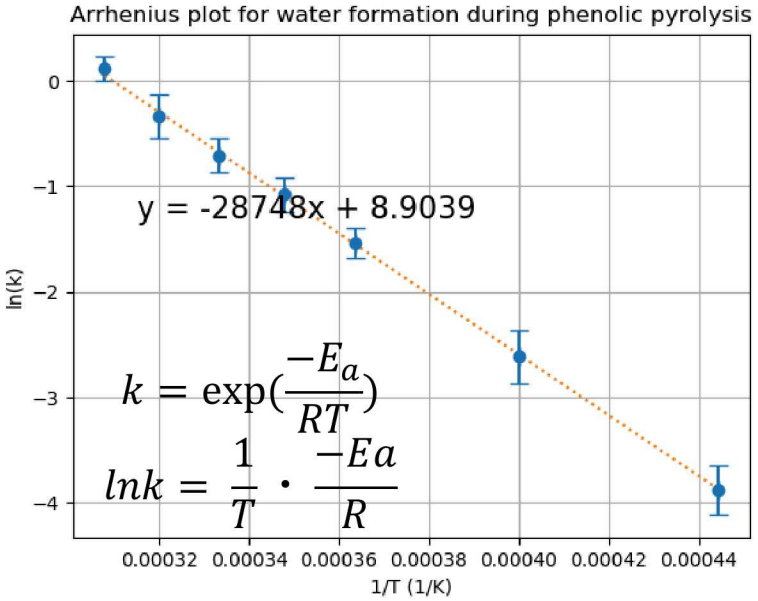

Methodology

1.) 16 linear chains – 15 instances.

2.) Product formation rates determined at various temperatures.

Water

-Abundant phenolic pyrolysis byproduct

-Formation kinetics studied with MD in the past.

Volatile species

-Closer proxy to experimentally determined activation energies based on thermogravimetric analysis (TGA).

-Mass cutoff(s) based on heaviest gaseous products observed experimentally.

3.) Activation energies (E_a) extracted using the Arrhenius equation

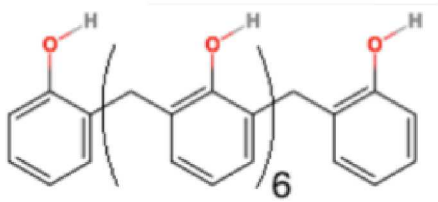

D. Jiang et al. *J. Phys. Chem. A* **113**, 6891-6894 (2009).
T. G. Desai et al. *Polymer* **52**, 577-585 (2011).
K. A. Trick et al. *Carbon* **33**(11), 1509-1515 (1995).
K. A. Lincoln *AIAA Journal* **21**(8), 1204 (1983).

Phenolic pyrolysis activation energies

NVT ensemble
1776 atoms – 16 linear phenolic chains
Periodic boundary conditions
15 instances
7-10 temperatures ranging from 2000 – 3250 K.
10s to 100s of ps per simulation
0.25 fs timestep

ρ = 1.25 g/cc	E_a (H_2O) (kj/mol)	E_a (Global) (kj/mol)	Source of variation
Exp, Jiang	----------	223-305	Temperature region and heating rates
Exp, Trick	----------	74-198	Temperature region and heating rates
Exp, Freidman	----------	192 - 293	Heating rate, method of determination
MD, Jiang	332 +/- 64	----------	
MD, Desai	286 +/- 46	----------	
This work, CHO	246 +/- 23	301 +/- 32	
This work, hybrid	172 +/- 22	206 +/- 23	
This work, Mattsson	130 +/- 6	191 +/- 13	

H. Jiang et al. *Carbon* **48**, 352-358 (2010).
K. A. Trick et al. *Carbon* **35**(3), 393-401 (1997).
H. L. Freidman *J. Polym. Sci. C* **6**(1), 183-195 (1964).
G. P. Shulman et al. *J. Appl. Polym. Sci.* **10**, 619-635 (1966).

All reax parametrizations agree with experiment – variation too great to constrain MD results, which vary.

Water formation pathways and energy barriers

The "Nudged Elastic Band" procedure, available in LAMMPS, was used to evaluate the activation energies for water formation with the hybrid and CHO ReaxFF parametrizations.

This procedure interpolates a set of structures between reactants and products and converges to the minimum energy path between them.

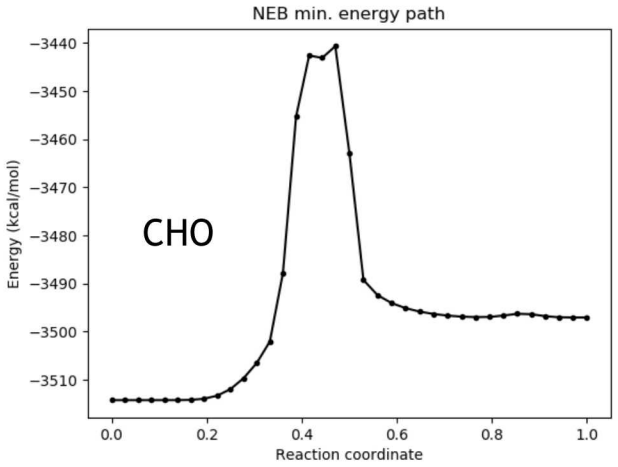

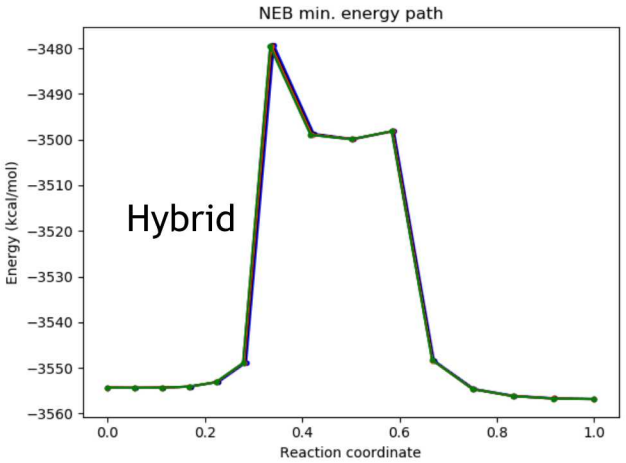

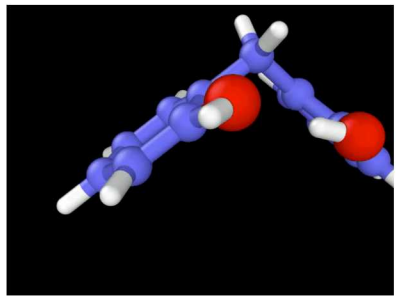

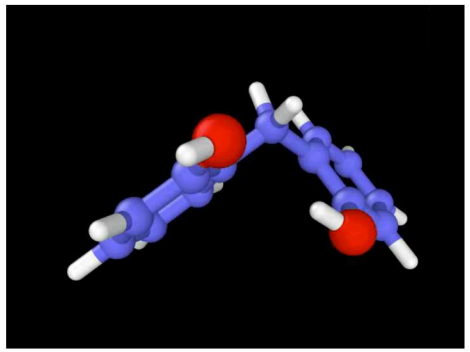

DFT transition state

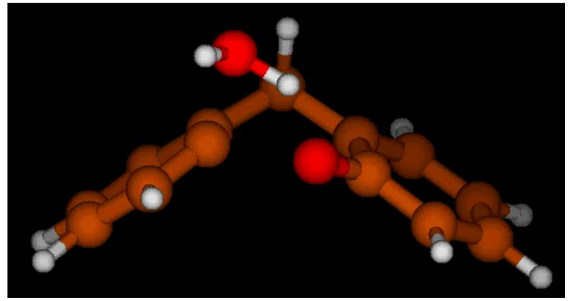

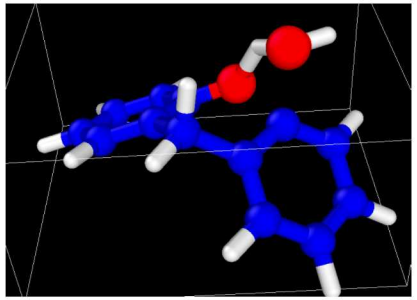

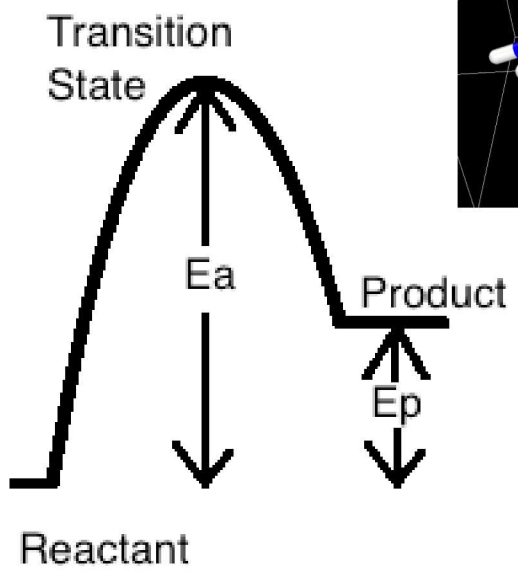

Intramolecular OH-OH water formation pathway – dimer

Water formation energies

Formulation	E_a (kcal/mol)	E_p (kcal/mol)
ReaxFF - hybrid	73.6	0.8
ReaxFF - CHO	73.6	----------
ReaxFF - CHO	85.8	25.1
DFT - B3LYP	67.9	5.8
CCSD(T)/6-31G**	70.9	6.1

C.W. Bauschlicher Jr. et al. *J. Phys. Chem. A* **117**, 11126 (2013).

Energy barrier with ReaxFF - CHO improves relative to DFT in comparison with previous work when using nudged elastic band, ReaxFF-optimized structures.

Previously calculated ReaxFF activation energies used DFT-optimized transition states.

-ReaxFF energy barriers agree with quantum chemical calculations within 3-6 kcal/mol.
-ReaxFF-hybrid product energy agrees within 5 kcal/mol with DFT.

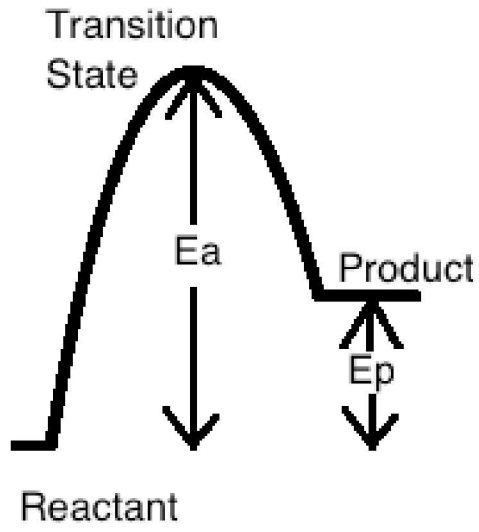

Conclusions and future work

1.) New hybrid ReaxFF parametrization most accurately represents intermolecular interactions relevant for phenolic polymers across a range of temperatures.

2.) ReaxFF accurately models pyrolysis, based on a comparison with experimental pyrolysis results and a single DFT water formation mechanism.

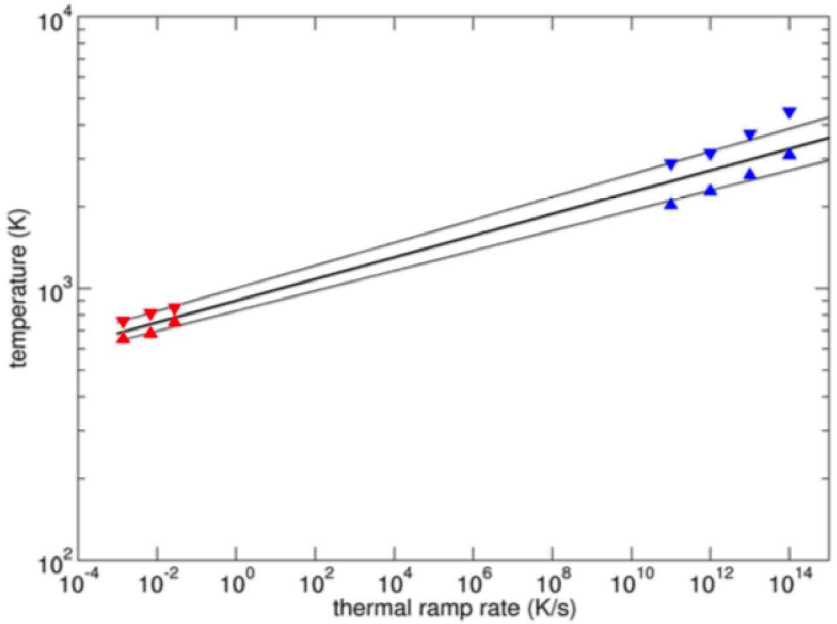

Image taken with permission:
J. M. D. Lane and N. W. Moore *J. Phys. Chem. A* **122**, 3962 (2018).

Acknowledgements

Sandia National Laboratories

High Performance Computers

NIST

Dr. Kenneth Kronlein

Bonus slide – DFT transition states

$\frac{\partial^2 E}{\partial x_1^2}$	$\frac{\partial^2 E}{\partial y_1 \partial x_1}$	…	$\frac{\partial^2 E}{\partial z_n \partial x_1}$
$\frac{\partial^2 E}{\partial x_1 \partial y_1}$	$\frac{\partial^2 E}{\partial y_1^2}$	…	$\frac{d^2 E}{\partial z_n \partial y_1}$
…	…	…	…
$\frac{\partial^2 E}{\partial x_1 \partial z_n}$	$\frac{\partial^2 E}{\partial y_1 \partial z_n}$	…	$\frac{\partial^2 E}{\partial z_n^2}$

3n x 3n Hessian (n = # of atoms) -
Diagonalization -> 3n pairs of eigenvalues and eigenvectors.

Eigenvectors – Vector of atomic displacements from converged geometry. Correspond to vibrational normal modes.
Eigenvalues – Proportional to square of vibrational frequency of corresponding mode.

- -All positive: System has converged to local minimum.
- -One negative: System has converged to first order saddle point.
  - May correspond to reasonable representation of transition state. Can be verified by visualization. Skill lies in pulling specific atoms out of equilibrium positions, such that optimizer converges to desired transition state.

E = system energy